Molecular dynamics of the rough sphere fluid. III. The dependence of translational and rotational motion on particle roughness[a)]

Charanjit S. Pangali and Bruce J. Berne

Department of Chemistry, Columbia University, New York, New York 10027
(Received 23 May 1977)

Molecular dynamics studies of two generalized forms of the rough sphere model are reported. The generalization permits us to vary the coupling between rotational and translational motion through a stick parameter λ. The autocorrelation functions show deviations from the Enskog theory for all values of λ studied—indicating that collective effects are involved. It appears that the angular velocity correlation function is the sum of two exponentials. A simulation of a mixture of disparate sized rough spheres was also performed. It is found that the rotational motion of the small particle is not significantly altered upon introduction of the large particles, but the linear velocity correlation function of the small particle differes considerably from that of the neat fluid (in the time regime from 5–15 mean collision time units).

I. INTRODUCTION

The rough sphere model[1] first proposed by Bryan is perhaps the simplest particle that has rotational degrees of freedom. A collision between two such particles is of zero duration and results in the interchange not only of linear momentum but also of angular momentum. Molecular dynamics studies of the rough sphere model have been reported previously.[2] In grazing collisions between two smooth spheres there is no scattering, whereas a grazing collision between two rough spheres can result in a large deflection angle. Rough spheres are therefore the "stickiest" possible particles. A number of schemes have recently been proposed to generalize the rough sphere model to handle molecules of an arbitrary degree or roughness. We shall consider the dynamics of two of these models: the rough domain model and the kinetic stick model. In both cases a parameter λ is introduced; $\lambda=0$ denotes pure slip, while $\lambda=1$ describes the usual rough sphere model. Taking $0<\lambda<1$ gives intermediate cases of slip.

The main purpose of this study is to provide data for a test of molecular hydrodynamics. In particular, we are interested in the relation between the boundary conditions to be used in molecular hydrodynamics and the microscopic collision dynamics. The results of the present study are discussed from this viewpoint in a companion paper[3] which follows this one. In this paper we discuss certain conclusions that can be immediately drawn from the data.

Section II describes the rough domain model, while Sec. III is devoted to a treatment of the kinetic stick model. In Sec. IV we describe the molecular dynamics method, which is followed by a section on the results for the rough domain model for a neat fluid for $\lambda=0$, 0.1, 0.25, 0.5, 0.75, 1.0. Section VI describes the results obtained for a single component fluid made up of molecules obeying the kinetic stick model. Some preliminary results obtained from a simulation of a mixture of rough spheres are described in Sec. VII, and in Sec. VIII we discuss the results.

[a)] This work was supported in part by grants from the National Science Foundation.

II. THE ROUGH DOMAIN MODEL

When two rough spheres labeled 1 and 2 with linear and angular velocities ($\mathbf{v}_1$, $\mathbf{v}_2$) and (ω_1, ω_2), respectively, collide the relative velocity of the points of contact on the surfaces of the colliding molecules $\mathbf{g}_{21}$ defined by

$$\mathbf{g}_{21}=\mathbf{v}_2-\mathbf{v}_1-\tfrac{1}{2}\hat{\mathbf{n}}\times(\sigma_2\omega_2+\sigma_1\omega_1) \tag{2.1}$$

is completely reversed by the collision, i.e.,

$$\mathbf{g}'_{21}=-\mathbf{g}_{21}. \tag{2.2}$$

Here $\hat{\mathbf{n}}$ denotes the unit vector along the line of centers of the colliding molecules and the prime denotes the relative velocity immediately after collision.

Recently, we have generalized the rough sphere model.[4] If $\mathbf{g}_{21}$ is resolved into a part parallel to the line of centers $\mathbf{g}_{\parallel}$ and a part perpendicular to this line $\mathbf{g}_{\perp}$, then the dynamical law can be expressed as

$$\mathbf{g}'_{\parallel}=-\mathbf{g}_{\parallel}, \tag{2.3a}$$

$$\mathbf{g}'_{\perp}=(1-2b_{21})\mathbf{g}_{\perp}, \tag{2.3b}$$

or

$$\mathbf{g}'_{21}=\mathbf{g}'_{\parallel}+\mathbf{g}'_{\perp}=-\mathbf{g}_{\parallel}+(1-2b_{21})\mathbf{g}_{\perp}, \tag{2.3c}$$

where $b_{21}=1$ for rough spheres and $b_{21}=0$ for smooth spheres.

Turning now to the rough domain model we imagine the surfaces of the two colliding spheres to be covered by domains of roughness separated by patches that are completely smooth. Furthermore, we assume that these patches are distributed randomly on the surface of a sphere. If α_1 is the fraction of the surface area of sphere 1 that is rough and α_2 the fraction of the surface area of sphere 2 that is rough, then the probability of having a completely sticky collision is given by $\alpha_1\alpha_2=b_{21}$. When $b_{21}=1$ the spheres upon collision obey the dynamical laws for rough spheres, while if $b_{21}=0$, the spheres upon collision obey the dynamical laws for smooth spheres. Intermediate cases of slip are obtained by taking $0<b_{21}<1$.

The collision dynamics of the rough domain model are completely determined by the laws of conservation of linear and angular momentum. If two such molecules,

 Copyright © 1977 American Institute of Physics

Downloaded 30 Dec 2003 to 128.59.114.15. Redistribution subject to AIP license or copyright, see http://ojps.aip.org/jcpo/jcpcr.jsp

labeled 1 and 2, with linear and angular velocities ($\mathbf{v}_1$, $\mathbf{v}_2$) and (ω_1, ω_2) collide, the velocities immediately after the collision are given by

$$\mathbf{v}_1' = \mathbf{v}_1 + 2M_2[(\kappa_0 + (1 - b_{21})\kappa_1\kappa_2)\,\hat{\mathbf{n}}\hat{\mathbf{n}}\cdot\mathbf{g}_{21} + b_{21}\kappa_1\kappa_2\mathbf{g}_{21}]/(\kappa_1\kappa_2 + \kappa_0), \tag{2.4}$$

$$\boldsymbol{\omega}_1' = \boldsymbol{\omega}_1 - 4M_2\kappa_2[b_{21}(\hat{\mathbf{n}}\times\mathbf{g}_{21})]/(\kappa_1\kappa_2 + \kappa_0)\,\sigma_1, \tag{2.5}$$

where $\hat{\mathbf{n}}$ is a unit vector pointing from the center of sphere 2 to the center of sphere 1 at contact, $M_2 = m_2/(m_1 + m_2)$, m_1 is the mass of sphere 1 and m_2 the mass of sphere 2, $\kappa_0 = M_1\kappa_1 + M_2\kappa_2$, and κ_1, κ_2 are the reduced moments of inertia defined as $\kappa_i = 4I_i/m_i\sigma_i^2$. Analogous equations apply for molecule 2. Here $b_{21} = 1$ for a rough contact and $b_{21} = 0$ for a smooth contact. When b_{21} is averaged over all collisions between particles of type 1 with particles of type 2 we obtain $\langle b_{21}\rangle = \lambda_{21}$.

It is a simple exercise to solve the Enskog equation for the transport coefficients of a partially rough sphere fluid. The shear viscosity of a neat fluid is (see Appendix B)

$$\eta_E = \lambda\,\eta_E(\text{rough}) + (1 - \lambda)\,\eta_E(\text{smooth}), \tag{2.6}$$

where the subscript E denotes the Enskog approximation. η_E(rough) is the viscosity in a purely rough sphere fluid and η_E(smooth) is the viscosity in a purely smooth hard sphere fluid. Because λ is the function of collisions which are rough, η_E is seen to be the mean value of the viscosity from rough and smooth collisions. The same kind of additivity holds for the other transport coefficients.

It is useful to consider the initial relaxation rates or Enskog rates $1/\tau_v(\alpha)$ and $1/\tau_\omega(\alpha)$ of the linear and angular velocity correlation functions, respectively, of particles of type α in a binary mixture. These are easily found to be

$$\frac{1}{\tau_v(\alpha)} = \sum_{\beta=1}^{2}\frac{1}{\tau_v(\alpha,\beta)}\,,\quad \frac{1}{\tau_\omega(\alpha)} = \sum_{\beta=1}^{2}\frac{1}{\tau_\omega(\alpha,\beta)}\,, \tag{2.7}$$

where $1/\tau_v(\alpha,\beta)$ and $1/\tau_\omega(\alpha,\beta)$ are the contributions from collisions of molecule of type α with molecules of type β:

$$\frac{1}{\tau_v(\alpha,\beta)} = 2M_\beta\left[\frac{\kappa_0^{\alpha\beta} + (1+\lambda_{\alpha\beta})\kappa_\alpha\kappa_\beta}{\kappa_\alpha\kappa_\beta + \kappa_0^{\alpha\beta}}\right]\Gamma_{\alpha\beta}, \tag{2.8}$$

$$\frac{1}{\tau_\omega(\alpha,\beta)} = \left(\frac{2M_\beta\kappa_\beta\lambda_{\alpha\beta}}{\kappa_\alpha\kappa_\beta + \kappa_0^{\alpha\beta}}\right)\Gamma_{\alpha\beta}\,, \tag{2.9}$$

where the quantities $\Gamma_{\alpha\beta}$ are

$$\Gamma_{\alpha\beta} = \frac{2\pi}{3}\,n_\beta g(\sigma_{\alpha\beta})\,\sigma_{\alpha\beta}^2\left(\frac{8k_BT}{\pi\mu_{\alpha\beta}}\right)^{1/2}, \tag{2.10}$$

where $\Gamma_{\alpha\beta}$ is $\frac{2}{3}$ times the collision frequency, $\sigma_{\alpha\beta} = \frac{1}{2}(\sigma_\alpha + \sigma_\beta)$, $\mu_{\alpha\beta}$ is the reduced mass of the particles, $g(\sigma_{\alpha\beta})$ is the contact pair correlation function, and n_β is the number density of component β.

In the case of a pure fluid these formulas reduce to

$$\frac{1}{\tau_v(\alpha,\beta)} = \frac{(1+\lambda)+1}{\kappa+1}\,\Gamma_{11} = \lambda\,\frac{1}{\tau_v(\text{rough})} + (1-\lambda)\,\frac{1}{\tau_v(\text{smooth})}\,, \tag{2.11}$$

$$\frac{1}{\tau_\omega(\alpha,\beta)} = \frac{\lambda}{\kappa+1}\,\Gamma_{11} = \lambda\,\frac{1}{\tau_\omega(\text{rough})} + (1-\lambda)\,\frac{1}{\tau_\omega(\text{smooth})}\,, \tag{2.12}$$

where $1/\tau_\omega$(smooth) is zero, $1/\tau_v$(rough) and $1/\tau_v$(smooth) are the linear velocity relaxation rates for fluids with $\lambda = 1$ and $\lambda = 0$, respectively, and $1/\tau_\omega$(rough) is the angular velocity relaxation rate for a fluid with $\lambda = 1$. Thus, the Enskog relaxation times are seen to be superpositions of the rough sphere and smooth sphere relaxation times—as were the transport coefficients.

These formulas will be useful for checking the accuracy of the molecular dynamics studies.

III. THE KINETIC STICK MODEL

The alternative model considered here is the kinetic stick model. According to this model we assume that when the relative kinetic energy along the line of centers exceeds a certain energy E_c, the collision is rough; otherwise, the collision is smooth. It is shown elsewhere that the fraction of collisions that are rough is given by[4]

$$\lambda_{21} = e^{-\beta E_c}\,, \tag{3.1}$$

where $\beta = 1/k_BT$. As in the case of the rough domain model λ_{21} varies from 0 (corresponding to perfect slip) to 1 (corresponding to perfect stick).

The initial slopes of correlation functions arising from this model are again given by Eqs. (2.11) and (2.12) (see Ref. 4), but the same kind of superpositions should not be expected for the transport coefficients because the dynamics of a molecule defined by the kinetic stock model will display much more correlation than the dynamics for a partially sticky molecule defined by the rough domain model. A hot molecule may be involved in a sequence of collisions that are all rough because the hot molecule may require many collisions before its energy relaxes to a value below E_c. In contrast to this, with the rough domain model collisions will alternate between rough and smooth in a completely random manner. The kinetic stick model does have the virtue that it is completely deterministic, i.e., the nature of a collision—whether rough or smooth—is determined by properties of the molecules, and not by some external source such as a random number generator. The rough domain model on the other hand lends itself more easily to theoretical treatment.

IV. MOLECULAR DYNAMICS METHOD

Given the simplicity of these models it would be of interest to test against them the tenets of molecular hydrodynamics. For this reason molecular dynamics calculations were performed for a series of λ values. The rough domain model was studied for $\lambda = 0.1$, 0.25, 0.5, and 0.75, while with the kinetic stick model $\lambda = 0.1$ and 0.5 were the systems simulated. In addition, we also simulated systems with $\lambda = 0$ and $\lambda = 1$.

The detailed comparisons with molecular hydrodynamics are presented in the accompanying paper.[3]

A system of 108 identical particles was simulated by

Downloaded 30 Dec 2003 to 128.59.114.15. Redistribution subject to AIP license or copyright, see http://ojps.aip.org/jcpo/jcpcr.jsp

the usual molecular dynamics methods.[2] The reduced density which is simply the number density expressed in units of the density at closest packing was 0.625. This corresponds to the liquid phase

$$\hat{\rho} \equiv \rho/\rho_{c.p.} = (\rho\sigma^3)/\sqrt{2}, \tag{4.1}$$

where ρ is the number density. Reduced units were employed in which the molecular mass is one, $k_BT = 1$ and the molecular radius is also one. The reduced moment of inertia κ can vary from 0 to 2/3. We chose $\kappa = 0.4$, which denotes a uniform distribution of mass over the sphere.

The nature of a collision for the rough domain model, i.e., whether it was to be rough or smooth, was determined by calling a random number generator (the IBM subroutine RANDU on the 360/370 series). This routine gives a sequence of numbers $\{\xi_i,\ i = 1, 2, 3, \ldots\}$ that are uniform in the interval (0, 1). If ξ_i was smaller than λ, then the collision dynamics were that of a rough sphere; otherwise, the collision was assumed to be between smooth spheres.

For the kinetic stick model the relative energy of approach $\frac{1}{2}\mu_{\alpha\beta}g_{\parallel}^2$ was computed; if this was greater than E_c [Eq. (3.1)], the collision was assumed to be rough.

Six runs of approximately 17000 collisions each were performed for a given λ and density. The phase point consisting of the linear and angular velocities was written on a direct access storage device at intervals of 1/4 mean collision time. Each run required approximately 10 minutes of CPU time. The value of the pair distribution function at contact $g(\sigma_{\alpha\beta})$ was computed during the dynamics run from

$$g_{\alpha\beta}(\sigma_{\alpha\beta}) = (Z_{\alpha\beta}V)/[2\pi N_\alpha(N_\beta - \delta_{\alpha\beta})\tau\sigma_{\alpha\beta}^3], \tag{4.2}$$

where V is the volume of the box, N_α and N_β are the number of particles of type α and β, respectively, τ is the length of the trajectory, and $Z_{\alpha\beta}$ is the virial corresponding to the pair α, β defined by[5]

$$Z_{\alpha\beta} = \sum_{\gamma=1}^{c(t)} m_\alpha \sigma_{\alpha\beta}(t_\gamma) \cdot \Delta \mathbf{V}_\alpha(t_\gamma), \tag{4.3}$$

where $\sigma_{\alpha\beta} = \sigma_{\alpha\beta}\hat{\mathbf{n}}$, with $\sigma_{\alpha\beta} = (\sigma_\alpha + \sigma_\beta)/2$, and $\Delta\mathbf{V}_\alpha(t_\gamma)$ is the change in the velocity of molecule α at the γth collision. For a binary mixture of particles α and β we can express the total pressure as

$$\frac{PV}{NkT} = 1 + \frac{P_{\alpha\alpha}V}{NkT} + \frac{P_{\alpha\beta}V}{NkT} + \frac{P_{\beta\beta}V}{NkT}, \tag{4.4}$$

where each individual pressure P_{ij} can be determined from

$$\frac{P_{ij}V}{NkT} = \frac{2}{2^{\delta_{ij}}}\left(\frac{2\pi}{3v}\right)\frac{N_i(N_j - \delta_{ij})}{N}\sigma_{ij}^3 g_{ij}(\sigma_{ij}). \tag{4.5}$$

In order to achieve good statistics in the simulation of the mixture a larger system was studied. At first, 256 uniform particles at $\hat{\rho} = 0.625$ were studied using the "cell method" of bookkeeping (see Appendix A). The initial configuration for our mixture was then obtained by selecting eight particles out of the 256 and swelling them to twice the radius of the remaining particles (see Appendix A). The density of the small particles was maintained at $\hat{\rho} = 0.625$. In this way the effect of the motion of large particles on the motion of small particles can best be studied. The simulation of the mixture was performed with both the small and big particle obeying the completely stick boundary conditions ($\lambda = 1$). Also, κ was maintained at 0.4 for both kinds of particles.

TABLE I. Initial slopes in mean collision times for the rough domain model.

	$1/\tau_v$		$1/\tau_\omega$	
λ	Exptl.	Theory[a]	Exptl.	Theory[b]
1.0	0.859	0.857	0.463	0.476
0.75	0.821	0.810	0.356	0.357
0.5	0.766	0.762	0.238	0.238
0.25	0.723	0.714	0.121	0.119
0.10	0.688	0.686	0.0488	0.0476
0.0	0.663	0.666	...	...

[a]Equation (2.11). [b]Equation (2.12).

V. RESULTS FOR THE ROUGH DOMAIN MODEL

According to the Enskog theory of dense fluids correlated binary collisions are ignored. If one derives the linear and angular velocity correlation functions making the same assumption, one obtains the Enskog correlation functions

$$C_v(t, \lambda) = e^{-|t|/\tau_{v(\lambda)}}, \tag{5.1}$$

$$C_\omega(t, \lambda) = e^{-|t|/\tau_{\omega(\lambda)}}, \tag{5.2}$$

where $\tau_v(\lambda)$ and $\tau_\omega(\lambda)$ are defined in Eqs. (2.11) and (2.12), respectively. We will first compare our results with these Enskog correlation functions.

Table I presents the initial slopes of the various time correlation functions (CF's) in the mean collision times (mct), along with the theoretical predictions from Eqs. (2.11) and (2.12):

$$\text{slope} = -\frac{1}{t}\log\frac{C(t)}{C(0)}, \tag{5.3}$$

where $C(t)$ was the very first point of the CF after $C(0)$; in our case this corresponded to the value of the CF at 1/4 mct. The uncertainty in the correlation functions is ± 0.003 independent of time. Deviations from the Enskog theory set in soon after such a time interval. In keeping with our previous notation[2] the velocity and angular velocity correlation times determined from initial slopes will be referred to as the *Enskog correlation times.*

The correlation times obtained by integrating the CF's are denoted by (area); these times are displayed in Table II. The data are in units of mct. The uncertainty in the areas is typically ± 0.025. Figure 1 shows how the areas converge to a steady state value. It takes on the order of 10–20 mean collision times for the plateau to be reached. It is clear from Fig. 2 that the experimental correlation functions deviate from the Enskog predicted forms. The nonexponential behavior of the correlation functions indicates the importance of correlated collisions (see below). On plotting the cor-

Downloaded 30 Dec 2003 to 128.59.114.15. Redistribution subject to AIP license or copyright, see http://ojps.aip.org/jcpo/jcpcr.jsp

TABLE II. Correlation times determined from the area for the rough domain model.

λ	τ_v (area) Positive portion	Negative portion	Total	τ_ω (area)	$g(\sigma)$
1.0	1.041	0.353	0.688	2.863	4.93 ± 0.05
0.75	1.101	0.279	0.822	3.707	4.93 ± 0.05
0.50	1.190	0.287	0.903	5.305	4.92 ± 0.05
0.25	1.276	0.238	1.038	10.450[a]	4.92 ± 0.05
0.10	1.341	0.213	1.128	23.250[a]	4.93 ± 0.05
0.0	1.410	0.161	1.249	···	4.92 ± 0.05

[a]It was found that the experimental data did not go to long enough times for the AVCF to have completely decayed to zero. The value reported here was obtained by extrapolating the area till a constant value resulted.

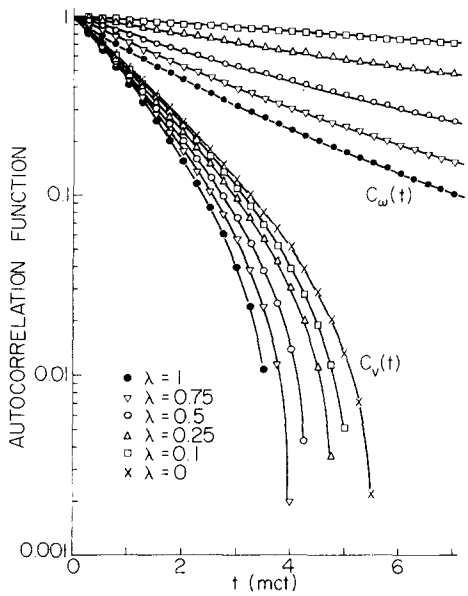

FIG. 2. The angular and linear velocity correlation functions for a series of the stick parameter λ on a semilog plot showing, respectively, the positive and negative deviations from the Enskog result. The Enskog curves (not shown) are just straight lines with slope given by Eqs. (2.11) and (2.12).

relation functions in units of the Enskog correlation times $\tau_\omega(\lambda)$ and $\tau_v(\lambda)$ (Fig. 3) we observe that the AVCF's for different λ's approximately coincide. However, the VCF's display deviations from each other after $t \sim 3\tau_v$ [Fig. 3(c)]. Therefore, collective effects are independent of λ as far as the AVCF's are concerned, but the same cannot be said for the VCF's. Note, however, that the minima in the VCF's in Fig. 3(c) occur at roughly the same point.

We find that the AVCF can be decomposed into a sum of two exponentials, the first decaying with the Enskog slope, and the second at a slightly smaller rate, approximately 0.8 times the Enskog slope.

The variation in shape and depth of the negative region of the VCF at a series of λ is shown in Fig. 4. With increasing λ the negative region increases, and the position of the minimum occurs at an earlier time. As noted earlier a grazing collision between two rough spheres can result in a large deflection angle. Hence, as λ increases we can anticipate a deeper minimum in the VCF. The areas arising from the positive and negative parts of the VCF are separately listed in Table II. The uncertainty in all these results is on the order of 1%; hence, our aim is to establish qualitative trends. Also in Table II we give the value of the pair distribution function at contact $g(\sigma)$. This function is independent of λ, as expected, and provides a reasonable check on the accuracy of the dynamics.

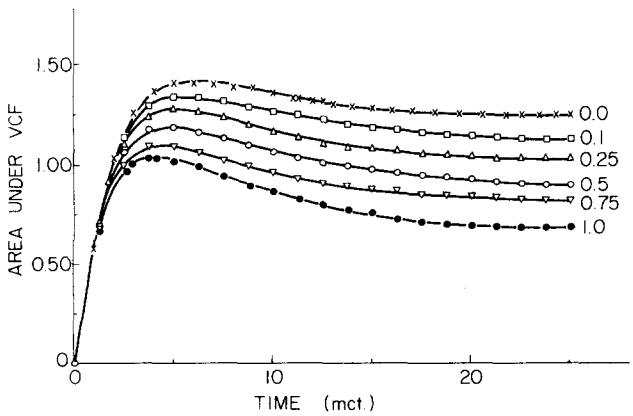

FIG. 1. The integral of the VCF as a function of the upper limit of integration for a series of the stick parameter λ. Time is measured in units of mean collision times (mct).

VI. RESULTS FOR THE KINETIC STICK MODEL

In contrast to the rough domain model (RDM), which required the use of a random number generator, the kinetic stick model (KSM) is completely deterministic. It remains to be shown which of these models corresponds more closely to physical reality. Table III summarizes the data obtained for the two cases (λ = 0.1, 0.50) studied using this model. Figure 5(b) shows that properties for the KSM scale in a very nonlinear fashion. In this context we note that in the negative region (in the time regime from 5–15 mct) $C_v(1,t) \leq C_v(\lambda,t) \leq C_v(0,t)$, but that as λ is varied from 0 to 1 $C_v(\lambda,t)$ approaches $C_v(1,t)$ much more rapidly in the KSM than in the RDM.

The errors in the correlation functions are small enough for us to conclude that the VCF's for a given λ do differ for the two models discussed here.

VII. MIXTURES

A mixture of eight particles of radius equal to twice that of the 248 solvent particles was simulated. The

TABLE III. Correlation times determined from the initial slope (Enskog) and from the area for the kinetic stick model.

λ	$1/\tau_v$	$1/\tau_\omega$	τ_v (area) Positive portion	Negative portion	Total	τ_ω (area)	$g(\sigma)$
0.50	0.764	0.233	1.168	0.328	0.840	5.093	4.95 ± 0.05
0.10	0.684	0.044	1.339	0.233	1.106	25.750[a]	4.91 ± 0.05

[a]See footnote for Table II.

Downloaded 30 Dec 2003 to 128.59.114.15. Redistribution subject to AIP license or copyright, see http://ojps.aip.org/jcpo/jcpcr.jsp

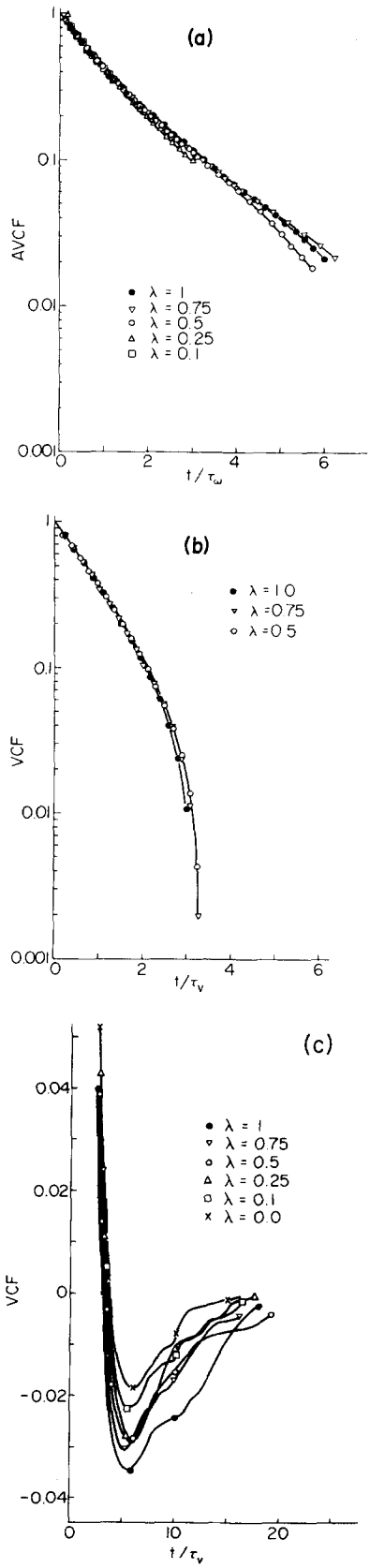

FIG. 3. (a) The angular velocity correlation functions are plotted vs reduced time (t/τ_ω), where τ_ω are the experimentally measured initial slopes given in Table I. (b) The linear velocity correlation functions plotted vs reduced time (t/τ_v), where τ_v are the initial slopes from experiment (see Table I). (c) The VCF's in (b) plotted on a different scale to show the negative region. See Fig. 4 for further comments.

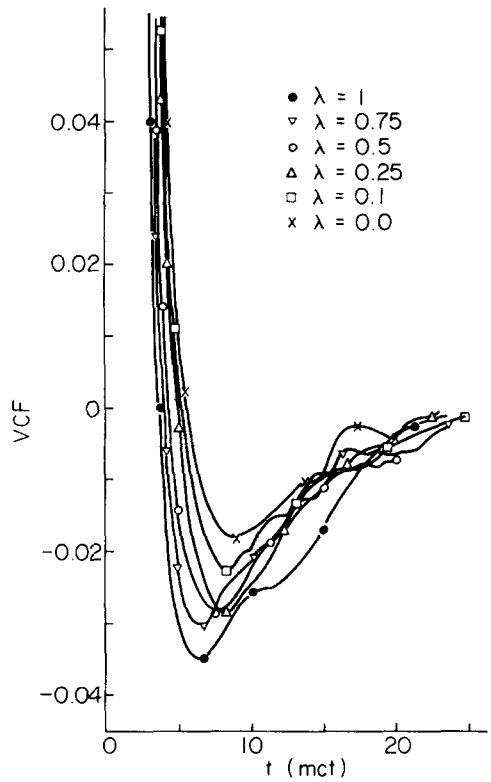

FIG. 4. The velocity autocorrelation functions measured in units of mean collision time. The uncertainty in the results is ±0.003. The points shown are not actual data points but a guide for the artist. Data points were obtained at intervals of 0.25 mct.

mass of the big particle was taken to be 8, while that for the small particle was 1. In both cases the mass was distributed uniformly in the spheres ($\kappa = 0.4$) and the stick parameter λ_{21} was set equal to 1.0. In these units the moment of inertia of the small particle is 0.4 while that of the big particle is 12.8. The density $\hat{\rho}$ of the small particles was 0.625 after excluded volume effects due to the big particles had been taken into account [the volume available to the small particles was taken to be that of the box minus the excluded volume of the big particles, the latter being $\frac{4}{3}\pi(\sigma_{SB}/2)^3 \times 8$]. The results of the mixture will be compared with a simulation of a neat fluid of 256 particles at a density $\hat{\rho} = 0.625$.

In Table IV we present the results for the pair correlation function and compare them with Percus–Yevick theory,[6] denoted by PY. The uncertainty in $g_{BB}(\sigma_{BB})$ is large (±0.80) because the trajectory was not long

TABLE IV. Collision rates and the contact pair distribution functions for the mixture.

α	β	$g_{\alpha\beta}(\sigma_{\alpha\beta})$	PY	$\Gamma^{\alpha\beta}_{MD}$	$\Gamma^{\alpha\beta}$
S	S	3.68±0.03	3.341	427.7	432.5[c]
S	B	4.63±0.33	3.885	59.46	59.46[c]
B	B	6.58±0.80	4.973	1[b]	1[c]

[a] S denotes the small particle and B denotes the big particle.
[b] The normalization constant for $\Gamma^{\alpha\beta}_{MD}$ is 226.
[c] Collision rates calculated from Eq. (7.1).

Downloaded 30 Dec 2003 to 128.59.114.15. Redistribution subject to AIP license or copyright, see http://ojps.aip.org/jcpo/jcpcr.jsp

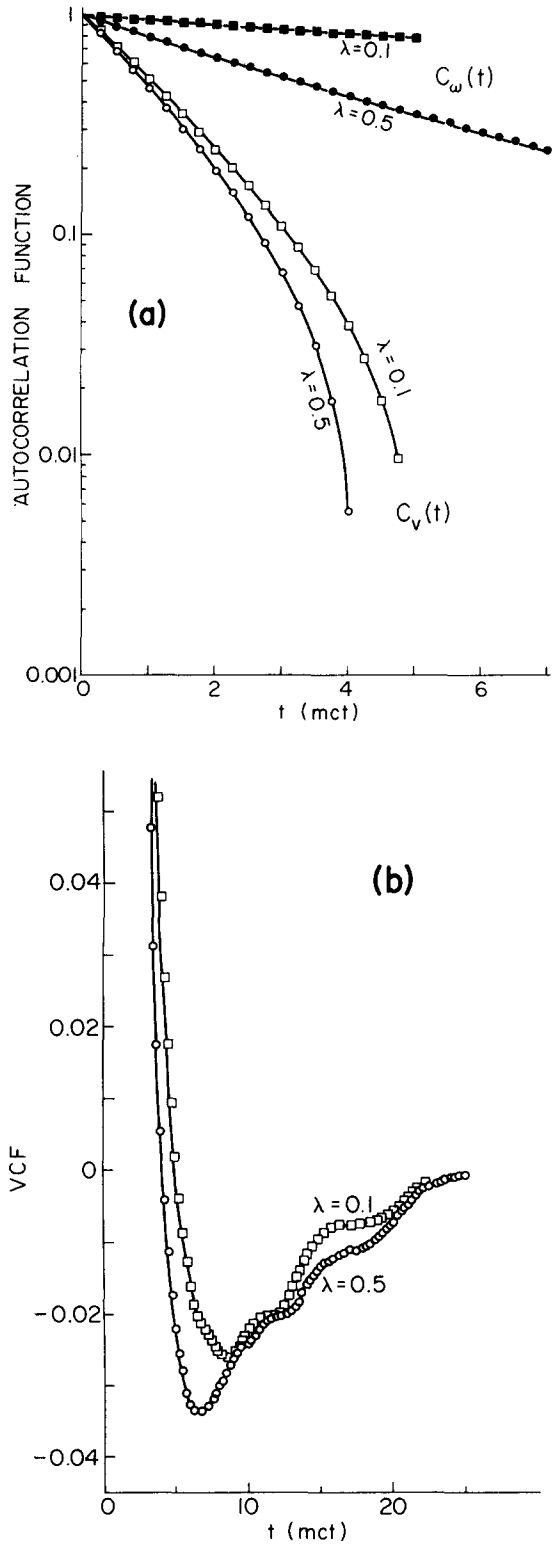

FIG. 5. (a) The angular and linear velocity correlation functions for the kinetic stick model. (b) The velocity correlation functions at $\lambda=0.1$ and $\lambda=0.5$, studied with the kinetic stick model. The uncertainty is again ± 0.003.

enough to sample very many collisions between big particles.

The Mansoori–Carnahan–Starling–Leland[7] (MCSL) equation of state gives the total pressure of the system as 0.572 (in reduced units) compared to the molecular dynamics value of 0.574 ± 0.005. The latter was determined from Eq. (4.4). The compressibility and virial forms of the Percus–Yevick equation of state yield 0.598 and 0.521, respectively, for the pressure. Thus, the MCSL equation of state, in contrast to the PY equations of state, provides a surprisingly accurate value of the total pressure of the system. Also given in Table IV are the collision rates for the different kinds of collisions; these are compared with the calculated rates using

$$\Gamma^{\alpha\beta} = (\tfrac{1}{2})^{\delta_{\alpha\beta}} \Gamma_{\alpha\beta}(N_\beta - \delta_{\alpha\beta}), \tag{7.1}$$

where $\Gamma^{\alpha\beta}$ gives the rate of collisions of molecules of type α with particles of type β and $\Gamma_{\alpha\beta}$ has been defined previously. The latter are normalized to give the correct value for big-particle collisions. In Table V we compare the experimental relaxation rates with those calculated from Eq. (2.7). They are given in units of the mct for small particles colliding with small particles. The agreement is seen to be extremely good. The areas obtained from integration of the autocorrelation functions are also given in Table V.

We have plotted the autocorrelation functions for the mixture in reduced units (Fig. 6). To facilitate a comparison with the results obtained for the neat fluid correlation functions for a simulation of 256 identical rough spheres at the same density as the solvent are also shown in Fig. 6. It is seen that the AVCF's for the neat fluid and for the small particles in the mixture very nearly coincide, indicating that the big particle has little or no effect on the rotational motion of the small particles. However, the VCF's do not coincide in the negative region. The negative region of the VCF for the small particles is significantly reduced, although the packing is unchanged, i.e., the density $\hat{\rho}$ of the small particles is still 0.625.

VIII. DISCUSSION

The rough sphere fluid has recently been studied by Mehaffey *et al.*[8] They present a renormalized kinetic theory for tagged particle motion in such a fluid which includes the effects of correlated collisions. The kinetic theory is able to account for all of the qualitative features of our results and moreover it provides considerable insight into the nature of the deviations of the VCF and AVCF from their predicted Enskog behavior. An examination of the various mode coupling contribu-

TABLE V. Correlation times for the mixture in units of the mean collision time for small particles colliding with small particles.

	$1/\tau_v(S)$[a]	$1/\tau_v(B)$	$1/\tau_\omega(S)$	$1/\tau_\omega(B)$
Exptl.	0.974	0.486	0.529	0.255
Theory [Eq. (2.7)]	0.961	0.474	0.534	0.263
Area[b]	1.357	0.417	0.448	0.229

[a]Symbols S and B denote the small particle and the big particle, respectively.
[b]In units of $(\text{mct})^{-1}$.

Downloaded 30 Dec 2003 to 128.59.114.15. Redistribution subject to AIP license or copyright, see http://ojps.aip.org/jcpo/jcpcr.jsp

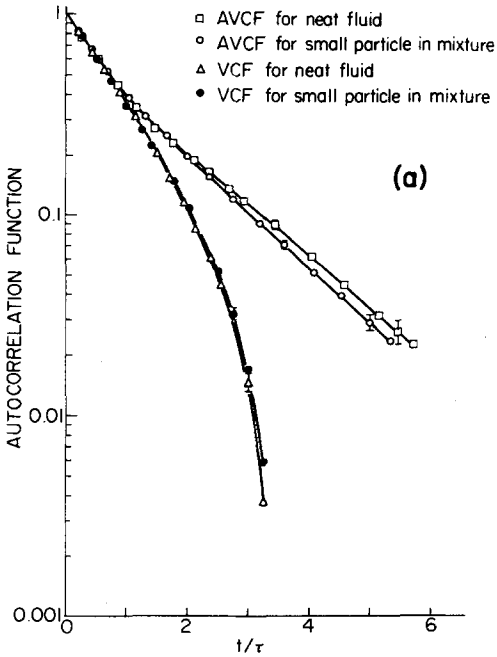

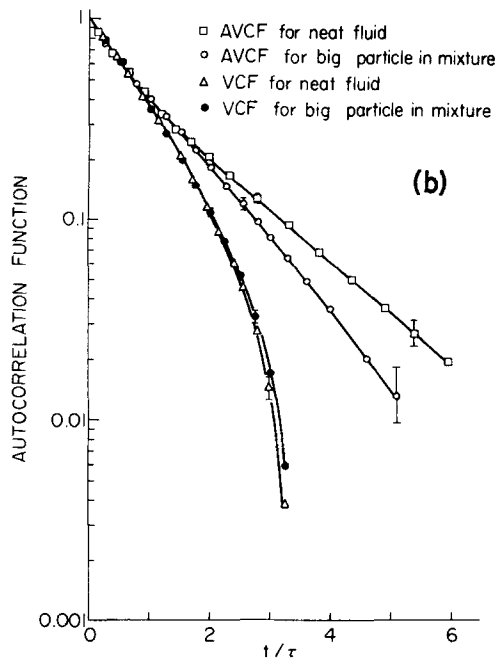

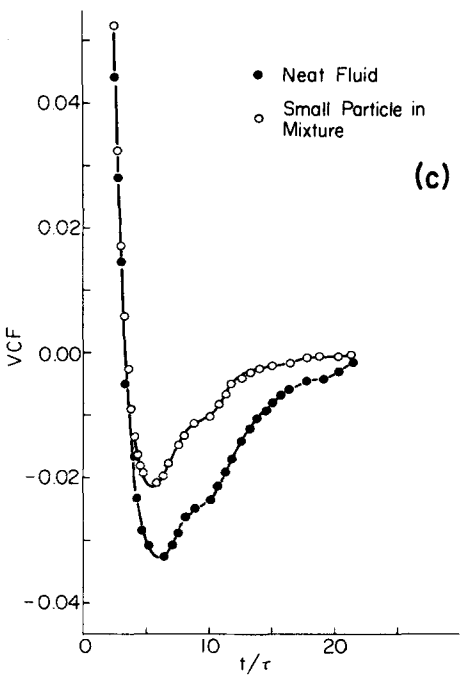

FIG. 6. (a) Comparison of the small particle motion in the mixture with results from a simulation of 256 identical rough spheres. The time is given in reduced units; $\tau = \tau_v$ for the VCF and $\tau = \tau_\omega$ for the AVCF. τ_v and τ_ω for the small particle are given in Table V, while for the neat fluid $1/\tau_v$ and $1/\tau_\omega$ were experimentally determined to be 0.862 and 0.476, respectively. (b) Comparison of the big particle motion in the mixture with results for a neat fluid of 256 particles. Symbols as in (a). (c) The linear velocity correlation functions in (a) drawn on a different scale to show the effect of packing. The abscissa denotes time in reduced units t/τ, where τ is the experimentally measured initial slope for $\lambda = 1$ in Table I.

tions reveals that for the VCF the coupling of the velocity to density fluctuations in the fluid dominates for short times and leads to a "cage" effect and an initial negative deviation from the Enskog form. On the other hand, the coupling to the transverse angular velocity fluctuations of the fluid dominates for short times in the case of AVCF leading to positive deviations from the Enskog theory; coupling to the longitudinal fluctuations of the fluid is precluded because of the symmetry of the rough sphere. The negative region of the VCF is ascribed to the coupling of the linear momentum of the tagged particle to the density fluctuations in the fluid. It would appear from Fig. 4 that this coupling increases with λ. In fact, we find that the negative region displays a rather complicated dependence on the stick parameter λ. The total area under the VCF very nearly goes as

$$1/\tau_v(\text{area}) = \lambda/\tau_v^R(\text{area}) + (1-\lambda)/\tau_v^S(\text{area}), \qquad (8.1)$$

where τ_v^R and τ_v^S refer to the areas under the VCF's for $\lambda = 1$ and $\lambda = 0$, respectively. However, although $\tau_\omega(\text{area})$ is an inverse function of λ, it does not simply depend on λ as $\tau_\omega(\text{area}) = \tau_\omega^R(\text{area})/\lambda$. The translational and rotational diffusion coefficients are related to $\tau_v(\text{area})$ and $\tau_\omega(\text{area})$ by $D_T = (kT/m)\,\tau_v(\text{area})$ and $D_R = (kT/I)\,\tau_\omega(\text{area})$. The dependence of the diffusion coefficients upon λ is displayed in Fig. 7.

The AVCF and the VCF are not simple superpositions of the rough and smooth sphere correlation functions, i.e., the relation

Downloaded 30 Dec 2003 to 128.59.114.15. Redistribution subject to AIP license or copyright, see http://ojps.aip.org/jcpo/jcpcr.jsp

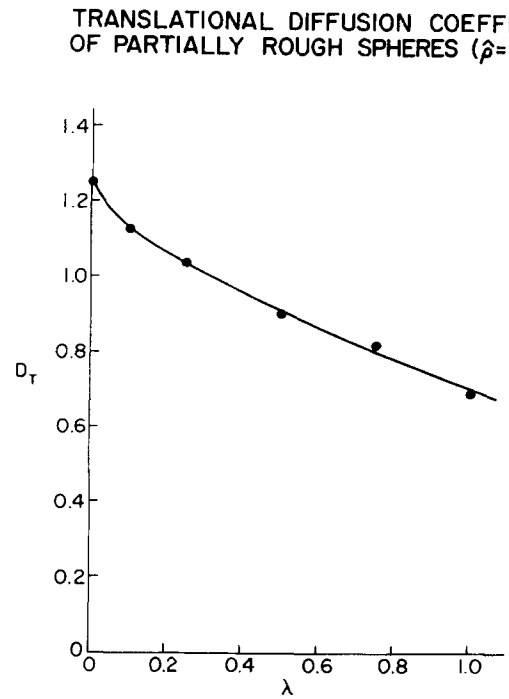

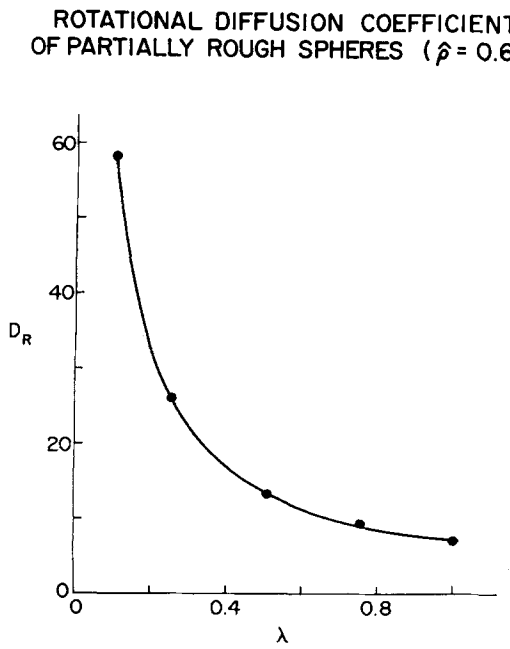

FIG. 7. (a) Dependence of the translational diffusion coefficient upon λ. D_T is given in reduced units where the mass of the particle is one, its radius is one, and time is measured in units of mean collision times. (b) Dependence of the rotational diffusion coefficient upon λ. D_R is the same reduced units as D_T [Fig. 7(a)].

$$C(t, \lambda) = C(t, \lambda = 1) + (1 - \lambda)\, C(t, \lambda = 0) \qquad (8.2)$$

is not obeyed. As seen from Fig. 3(a), the AVCF appears to be very clearly a sum of two exponentials, the first one having the Enskog slope and the second a slightly smaller slope. The VCF displays a more complicated behavior in contrast to the AVCF [Fig. 3(b)].

The kinetic stick model shows features quite distinct from the rough domain model. In particular, the VCF for moderate values of λ (e.g., λ = 0.5) approaches that for λ = 1 in the time regime from 5–15 mct.

Finally, the results from the simulation of a mixture of disparate sized rough spheres reveal that the AVCF of the solvent particles is not significantly altered upon introduction of large particles. Although it might appear that around $t = 4 - 5\tau_\omega$ the two AVCF curves in Fig. 6(a) differ, it must be pointed out that the accuracy in this region is small (as indicated by the error bars). However, a change in packing has a more profound effect on the VCF of the solvent particles [Fig. 6(c)]. This is not altogether surprising since back-scattering events which are of greater importance in the study of the VCF than the AVCF[8] are likely to be altered in the presence of the large particles. It appears from Fig. 6(c) that the presence of the large particles diminishes the coupling of the linear momentum of the solvent particles to the density fluctuations in the fluid.

The data reported here will be used to test hydrodynamic theories of the angular velocity correlation function and the concept of particle roughness.[3]

APPENDIX A. PROGRAMMING TECHNIQUES

The molecular dynamics (MD) technique used here computes the trajectory of hard-core particles, subject to periodic boundary conditions. For an excellent didactic exposition of the method see the treatment given by Erpenbeck and Wood.[5] We describe here the bookkeeping method used for our code.[9] Two lists of neighboring cells were enacted. In the first the neighbors of each cell were listed such that no two cells were counted as neighbors more than once. This list was used to initialize the program. After a collision has occurred one needs to recompute only the collision times for the molecules involved in the collision with the rest of the particles. The second list gave the 26 neighboring cells for the cell containing one (or both) of these molecules, so that once a collision had occurred the code identified the cell containing the colliding particle (or particles) and then proceeded to compute fresh collision times with particles in that cell and in the neighboring 26 cells. The region required for these two lists was found to be nominal.

A few words on the swelling procedure used for generating the initial configuration of the mixture would be in order. First, the box containing the 256 particles was expanded to the required size. Then eight of the particles were selected at random and identified for the swelling. A list of collision times was drawn up and the shortest collision time t_m selected. The system was advanced in time by $\frac{1}{2}t_m$ and the distances between the eight particles and their nearest neighbor particles calculated. The smallest of these distances γ_s was selected and the radius of the eight particles was increased by $\sim\gamma_s/2$. Fresh collision times were computed and a collision performed. The procedure was now repeated by computing collision times, finding t_m, advancing by $t_m/2$, etc. until the radius of the eight selected particles reached the desired value.

Downloaded 30 Dec 2003 to 128.59.114.15. Redistribution subject to AIP license or copyright, see http://ojps.aip.org/jcpo/jcpcr.jsp

APPENDIX B

Let us first consider the binary collision operator T_{ij} for a collision between a molecule i and j. If the collision is rough $T_{ij} = T^R_{ij}$, whereas if it is smooth $T_{ij} = T^S_{ij}$. This allows us to write

$$T_{ij} = b_{ij} T^R_{ij} + (1 - b_{ij}) T^S_{ij} = T_{ij}(b_{ij}), \tag{B1}$$

where $b_{ij} = 1$ if the collision is rough and $b_{ij} = 0$ if the collision is smooth. Thus, the T operator $T_{ij}(b_{ij})$ is a linear function of b_{ij}.

The total Liouville operator L is

$$L = L_0 - \sum_{i>j} T_{ij}(b_{ij}), \tag{B2}$$

where L_0 is the free particle Liouvillian and the sum goes over all pairs of particles.

In the rough domain model a collision is rough or smooth depending on the value of b_{ij} sampled. For each collision the value of b_{ij} is sampled independently and the average value of b_{ij} is $\langle b_{ij} \rangle = \lambda$. Thus, the various b_{ij}'s are statistically independent.

In order to formulate the dynamics of the rough domain model, we must use the theory of stochastic Liouville equations. First note that the resolvent or Green's operator is

$$G(z^*) = \frac{1}{z - L + i\eta} . \tag{B3}$$

Substitution of Eq. (B1) in (B3) gives after obvious operator manipulations

$$G(z^*) = G_0(z^*) + \sum_{i>j} G_0(z^*)\, T_{ij}(b_{ij})\, G_0(z^*) + \sum_{i>j} \sum_{k>1}{}' G_0(z^*)\, T_{ij}(b_{ij})\, G_0(z^*)\, \Gamma_{kl}(b_{kl})\, G_0(z^*) + \ldots , \tag{B4}$$

where $G_0(z^*) = (E - L_0 + i\eta)^{-1}$ is the free particle Green's operator and where adjacent T's can't involve the same pairs [i.e., $(i,j) \neq (k,1)$]. Let $G(z^*)$ be the average Green's operator, i.e., the operator averaged over the independent random variables b_{ij}. Since $G_0(z^*)$ doesn't depend on the b's, it follows that

$$\bar{G}(z^*) = G_0(z^*) + \sum_{i>j} G_0(z^*)\, \bar{T}_{ij} G_0(z^*) + \sum_{i>j} \sum_{k>1}{}' G_0(z^*)\, \bar{T}_{ij} G_0(z^*)\, \bar{T}_{kl} G_0(z^*) + \ldots , \tag{B5}$$

where the average T operators are given by

$$\bar{T}_{ij} = T^R_{ij} + (1 - \lambda) T^S_{ij} . \tag{B6}$$

Thus, Eq. (B5) may be resumed to give

$$\bar{G}(z^*) = \left(z - L_0 - \sum_{i>j} \bar{T}_{ij} + i\eta \right)^{-1} . \tag{B7}$$

This shows that the Liouvillian for the rough domain model contains the average T operators. Standard tricks may now be employed to derive the Boltzmann–Enskog equation[1]

$$\left(\frac{\partial}{\partial t} + V_1 \cdot \nabla + m^{-1} \mathbf{F} \cdot \frac{\partial}{\partial V_1} \right) f_1 = \lambda \int\int\int (\mathbf{g}_{21} \cdot \hat{\kappa})\, \sigma\, (f_1' f_2' - f_1 f_2)\, d\kappa\, d\omega_2\, d\mathbf{V}_2 + (1 - \lambda) \int\int (\mathbf{g}_{21} \cdot \hat{\kappa})\, \sigma\, (f_1' f_2' - f_1 f_2)\, d\hat{\kappa}\, d\mathbf{V}_2 . \tag{B8}$$

Here $\mathbf{F} = \mathbf{F}(\mathbf{r})$ is the external force upon a molecule with center of mass at $\mathbf{r}$, $f_i = f(\mathbf{r}, \mathbf{V}_i, \omega_i; t)$ is the singlet distribution function prior to a collision, and $f_i' \equiv f(\mathbf{r}, \mathbf{V}_i', \omega_i'; t)$, where the primed variables are defined by Eqs. (2.4) and (2.5). Solving Eq. (B8) in the manner outlined in Chapman and Cowling (Ref. 1) we obtain the desired result [Eq. (2.6)]

$$\eta_E = \lambda \eta_R + (1 - \lambda) \eta_S . \tag{B9}$$

Similar results apply to all other transport coefficients.

[1] S. Chapman and T. G. Cowling, *The Mathematical Theory of Non-Uniform Gases* (Cambridge University, Cambridge, 1960).

[2] J. O'Dell and B. J. Berne, J. Chem. Phys. **63**, 2376 (1975); see also G. Subramanian and H. Ted Davis, Phys. Rev. A **11**, 1430 (1975).

[3] J. Montogomery and B. J. Berne, J. Chem. Phys. **67**, 4580 (1977), following article.

[4] B. J. Berne, J. Chem. Phys. **66**, 2821 (1977).

[5] J. J. Erpenbeck and W. W. Wood, *Modern Theoretical Chemistry*, edited by B. J. Berne (Plenum, New York, 1977), Vol. VI.

[6] J. L. Lebowitz, Phys. Rev. A **133**, 895 (1964).

[7] G. A. Mansoori, N. F. Carnahan, K. E. Starling, and T. W. Leland Jr., J. Chem. Phys. **54**, 1523 (1971).

[8] J. R. Mehaffey, R. C. Desai, and R. Kapral, J. Chem. Phys. **66**, 1665 (1977).

[9] The bookkeeping scheme used in our code was an adaptation from a scheme devised by L. Nady.

Downloaded 30 Dec 2003 to 128.59.114.15. Redistribution subject to AIP license or copyright, see http://ojps.aip.org/jcpo/jcpcr.jsp